Redox Biology 6 (2015) 552–564

Contents lists available at ScienceDirect

Redox Biology

journal homepage: www.elsevier.com/locate/redox

Research Paper

Critical role of c-jun *N*-terminal protein kinase in promoting mitochondrial dysfunction and acute liver injury

Sehwan Jang [a,1], Li-Rong Yu [b,1], Mohamed A. Abdelmegeed [a], Yuan Gao [b], Atrayee Banerjee [a], Byoung-Joon Song [a,*]

[a] Laboratory of Membrane Biochemistry and Biophysics, National Institute on Alcohol Abuse and Alcoholism, Bethesda, MD 20892-9410, USA
[b] Biomarkers and Alternative Models Branch, Division of Systems Biology, National Center for Toxicological Research, Food and Drug Administration, Jefferson, AR 72079, USA

ARTICLE INFO

Article history:
Received 23 September 2015
Accepted 29 September 2015
Available online 9 October 2015

Keywords:
Acute liver injury
Carbon tetrachloride
JNK
Protein phosphorylation
Mitochondria
Differential proteomics

ABSTRACT

The mechanism by which c-Jun *N*-terminal protein kinase (JNK) promotes tissue injury is poorly understood. Thus we aimed at studying the roles of JNK and its phospho-target proteins in mouse models of acute liver injury. Young male mice were exposed to a single dose of CCl_4 (50 mg/kg, IP) and euthanized at different time points. Liver histology, blood alanine aminotransferase, and other enzyme activities were measured in CCl_4-exposed mice without or with the highly-specific JNK inhibitors. Phosphoproteins were purified from control or CCl_4-exposed mice and analyzed by differential mass-spectrometry followed by further characterizations of immunoprecipitation and activity measurements. JNK was activated within 1 h while liver damage was maximal at 24 h post-CCl_4 injection. Markedly increased phosphorylation of many mitochondrial proteins was observed between 1 and 8 h following CCl_4 exposure. Pretreatment with the selective JNK inhibitor SU3327 or the mitochondria-targeted antioxidant mito-TEMPO markedly reduced the levels of p-JNK, mitochondrial phosphoproteins and liver damage in CCl_4-exposed mice. Differential proteomic analysis identified many phosphorylated mitochondrial proteins involved in anti-oxidant defense, electron transfer, energy supply, fatty acid oxidation, etc. Aldehyde dehydrogenase, NADH-ubiquinone oxidoreductase, and α-ketoglutarate dehydrogenase were phosphorylated in CCl_4-exposed mice but dephosphorylated after SU3327 pretreatment. Consistently, the suppressed activities of these enzymes were restored by SU3327 pretreatment in CCl_4-exposed mice. These data provide a novel mechanism by which JNK, rapidly activated by CCl_4, promotes mitochondrial dysfunction and acute hepatotoxicity through robust phosphorylation of numerous mitochondrial proteins.

Published by Elsevier B.V. This is an open access article under the CC BY-NC-ND license (http://creativecommons.org/licenses/by-nc-nd/4.0/).

1. . Introduction

Epidemiological studies revealed that many people suffer from acute liver failure, which can be produced by overdose of potentially toxic compounds such as acetaminophen (APAP), cocaine, and binge alcohol (ethanol). For instance, over 56,000 emergency room visits with more than 400 deaths per year are due to APAP-induced acute liver injury in the United States alone [1]. Over-exposure to these substances can cause cell/tissue injury and sudden deaths in humans and experimental models [1,2 and references within] especially in combination with alcohol through additive or synergistic interactions [3,4]. However, the molecular mechanisms of acute liver damage by these agents remain elusive because of the conflicting results.

Carbon tetrachloride (CCl_4) is a hepatotoxic solvent widely used to study the mechanisms for acute liver injury and chronic fibrosis in experimental models [5–8]. The majority of CCl_4 is metabolized by the ethanol-inducible CYP2E1 and thus *Cyp2e1*-null mice are protected from CCl_4-induced liver damage [9]. Following CYP2E1-related metabolism, free radical metabolites of CCl_4 attack cellular membranes, producing lipid peroxides, leading to severe necrosis in the pericentral regions of the liver [5,6]. However, despite the

Abbreviations: ALT, alanine aminotransferase; APAP, acetaminophen; CYP2E1, cytochrome P450 2E1; ERK, extracellular signal-regulated kinase; α-KGDH, α-ketoglutarate dehydrogenase; HAE, 4-hydroxyalkenal; JNK, c-Jun *N*-terminal protein kinase; MDA, malondialdehyde; MPT, mitochondrial permeability transition; NdufS1, 75 kDa-subunit NAD^+-dependent ubiquinone-oxidoreductase; p38K, p38 kinase; PBS, phosphate buffered saline; PDH, pyruvate dehydrogenase; TNF-α, tumor necrosis factor-alpha; WT, wild-type

* Corresponding author. Fax: +1 301 594 3113.
E-mail addresses: sehwan.jang@upr.edu (S. Jang), Lirong.Yu@fda.hhs.gov (L.-R. Yu), abdelmegeedm@mail.nih.gov (M.A. Abdelmegeed), yuangao2000@gmail.com (Y. Gao), atrayee.liver@gmail.com (A. Banerjee), bj.song@nih.gov (B.-J. Song).

[1] These authors equally contribute to this manuscript.

http://dx.doi.org/10.1016/j.redox.2015.09.040
2213-2317/Published by Elsevier B.V. This is an open access article under the CC BY-NC-ND license (http://creativecommons.org/licenses/by-nc-nd/4.0/).

well-established role of lipid peroxidation in this model [5,6], it is virtually unknown whether CCl_4 can promote liver injury through modifying the phosphorylation of cellular proteins.

Mitogen-activated protein kinases (MAPKs) are cell signal-related kinases known to regulate cell death and growth, depending on the cellular contexts and their temporal fluctuations. It is well-established that there are three major MAPKs: c-Jun *N*-terminal protein kinase (JNK), p38 kinase (p38K), and extracellular signal-regulated kinase (ERK). In general, activation of JNK and p38K is related to cell death signaling pathways while ERK activation is involved in cell survival and proliferation [10]. JNK-related signaling pathways are also known to be associated with liver physiology and pathology [11]. For instance, JNK-mediated cell damage has been observed with many toxic compounds such as APAP [12–14], staurosporine [15] and UV exposure [15] as well as under pathological conditions including ischemia-reperfusion injury [16]. Mendelson et al. [17] reported that JNK was potently activated while ERK and p38K remained unchanged and decreased, respectively, following CCl_4 treatment, suggesting a role of JNK in promoting hepatotoxicity. In contrast, other investigators reported that JNK activation was not critical in CCl_4-mediated acute liver injury, compared to the important role of JNK in APAP-induced liver damage [12,13]. Therefore, the underlying mechanism by which activated (phosphorylated) p-JNK promotes cell or liver damage is poorly understood.

We recently reported that CCl_4 rapidly activated p-JNK, which was translocated to mitochondria and phosphorylated mitochondrial aldehyde dehydrogenase (ALDH2), an anti-oxidant enzyme, leading to its inactivation and accumulation of lipid peroxides following CCl_4 exposure [18]. In addition, a previous report with isolated mitochondrial proteins showed that activated p-JNK phosphorylated other mitochondrial enzymes such as pyruvate dehydrogenase (PDH) E1α and β subunits, ATP synthase α and β subunits, and heat shock proteins (Hsp60 and Hsp70) [19]. Based on these reports, we hypothesized that p-JNK, rapidly activated at early hours after CCl_4 exposure, translocates to mitochondria, phosphorylates many mitochondrial proteins and suppresses their functions, contributing to mitochondrial dysfunction and necrotic liver damage. However, it is poorly understood how many other proteins are phosphorylated by p-JNK and whether these phosphoproteins are functionally altered to contribute to CCl_4-induced liver injury. Thus, we investigated the mechanism of acute hepatotoxicity by determining the role of JNK in promoting mitochondrial dysfunction and liver necrosis. For this purpose, we specifically aimed to identify and characterize mitochondrial JNK-target proteins in the absence or presence of the specific JNK inhibitors. To further support the role of JNK in causing hepatotoxicity, we also evaluated the histological and biochemical measurements of CCl_4-exposed *Cyp2e1*-null mice as compared to those of the corresponding wild-type (WT) counterparts.

2. Materials and methods

2.1. Chemicals and other materials

NAD^+ and propionyl aldehyde were purchased from Sigma (St. Louis, MO, USA). Specific antibodies to c-Jun, phospho-c-Jun (Ser63), JNK, phospho-JNK (Thr183/Tyr185), p38 kinase, phospho-p38 kinase (Thr180/Tyr182), ERK, phospho-ERK (Thr202/Tyr204), phospho-Ser-Pro, Bax, and cytochrome C were purchased from Cell Signaling Technology, Inc (Beverly, MA). Phosphoprotein-purification kit including the metal-affinity columns was obtained from Qiagen (Valencia, CA). ProQ-Diamond phosphoprotein staining reagent was from Invitrogen (Eugene, OR). Specific goat polyclonal antibodies to mitochondrial ALDH2, 75-kDa subunit (Ndufs1) of NADH-ubiquinone oxidoreductase (complex I), cytochrome c oxidase (complex IV), ATP synthase beta-subunit (ATP5B, complex V), lamin, α-tubulin, peroxiredoxin, and α-ketoglutarate dehydrogenase (α-KGDH) were obtained from Santa Cruz Biotechnology, Inc (Santa Cruz, CA, USA). Specific antibodies to 3-nitro-Tyr (3-NT) were from Abcam (Cambridge, MA) while specific anti-HNE-adducts were purchased from Calbiochem (La Jolla, CA, USA). Specific JNK inhibitors SU3327 [20] and BI-78D3 [21] were purchased from Tocris Bioscience (Bristol, United Kingdom). Both SU3327 and BI-78D3 inhibit JNK activity through blockade of protein-protein interaction between JNK and its scaffolding protein JNK-interacting protein-1 (JIP-1). In addition, another report suggested that BI-78D3 can inhibit JNK activity through covalent modification of Cys163 of JNK [22]. Other agents including the JNK inhibitor SP600125 and the mitochondria-targeted antioxidant mito-TEMPO [2-(2,2,6,6-tetramethylpiperidine-1-oxyl-4-ylamino) 2-oxoethyl]tripphenylphosphenium chloride [23] were obtained from Sigma (St. Louis, MO, USA).

2.2. Animal treatment and histological analysis

Age and gender-matched young male NCI-WT mice (Svj-129 background) and *Cyp2e1*-null mice [24], kindly provided by Dr. Frank J. Gonzalez (National Cancer Institute, Bethesda, MD), were used and kept in a 12 h light-dark cycle with food and water *ad libitum* in accordance with NIH guidelines. After a single intraperitoneal injection of CCl_4 (50 mg/kg as 0.5% in corn oil), the WT and *Cyp2e1*-null mice ($n=4$–5/group) were euthanized at the indicated time points. Each JNK inhibitor (10 mg/kg, a single ip injection, $n=4$–5/group) was prepared as 1.25 mg/mL with 10% Solutol-HS15 in PBS, and administered 30 min prior to CCl_4 injection. Mito-TEMPO was dissolved in sterile saline and administered by a single dose at 5 mg/kg ip 30 min before CCl_4 treatment. A portion from the largest lobe of each liver, obtained from CCl_4-exposed WT in the absence or presence of JNK inhibitors and *Cyp2e1*-null mice collected at different time points, was fixed in 10% neutral buffered formalin. After paraffin embedding and the cutting of 4 μm slices, all sections were stained with hematoxylin and eosin (H&E), as described [24]. Histological evaluation was performed in a blinded manner.

2.3. Mass spectrometry analysis of purified phosphorylated proteins

To affinity-purify phosphorylated proteins, 250 mg of mitochondrial proteins from WT mice at 2 h post-injection of CCl_4, were subjected to a metal-affinity column (Qiagen, Valencia, CA) by following the manufacturer's instructions. The purification procedures for vehicle-control (control) and CCl_4-exposed samples, respectively, were repeated at least five times to collect sufficient amounts of purified phosphoproteins. Purified phosphoproteins were resolved on 1-D SDS-PAGE. Each gel lane was cut with a razor blade into 13 bands, transferred into clean tubes and subjected to further digestion with sequencing grade trypsin (Promega, Madison, WI, USA). In-gel digestion of protein gel slices, nanoflow reversed-phase liquid chromatography (nanoRPLC)–tandem mass spectrometry (MS/MS) and protein identification analyses were performed as recently described [25]. For mass spectrometry analysis, each sample was re-dissolved in 15 μL of 0.1% formic acid and 5 μL was injected onto a 9 cm × 75 μm i.d. in-house packed fused silica capillary electrospray ionization (ESI) C18 column, which was coupled online to a liner ion trap mass spectrometer (LTQ XL, Thermo Electron, San Jose, CA). Peptide separation was performed at a flow rate of ~250 nL/min using a step gradient of 2–42% solvent B (0.1% formic acid in acetonitrile) for 40 min, 42–98% solvent B for 10 min, and 98% solvent B for 5 min. Both solvents A (0.1% formic acid in water) and B were

delivered by an Agilent 1200 nanoflow LC system (Agilent Technologies, Palo Alto, CA). The mass spectrometer was operated in a data dependent mode in which each full MS scan was followed by 7 MS/MS scans where the 7 most abundant peptide molecular ions were dynamically selected from the prior MS scan for collision-induced dissociation (CID) using a normalized collision energy of 35%. The raw MS/MS data were searched using the SEQUEST cluster running under BioWorks (Rev. 3.3.1 SP1) (Thermo Electron, San Jose, CA) against a mouse IPI proteome database downloaded from the European Bioinformatics Institute (EBI) (http://www.ebi.ac.uk) for the identification of peptides and proteins within each gel band. To identify phosphoproteins from CCl_4-exposed samples, only the proteins with two or more unique peptides were considered confidently as legitimate identifications. Subtraction of phosphoproteins between control and CCl_4-exposed samples was performed to further identify the proteins preferentially phosphorylated by CCl_4 exposure [26] using the similar method described previously [27]. For this analysis, the area of extracted ion chromatogram of each identified peptide was calculated. The total area of all the peptides identified from the same protein was then normalized by the total area of all the proteins identified within the sample (13 gel bands for each sample) and expressed as parts per million (ppm) that referred to normalized intensity. After normalization, a ratio was calculated for each protein between the CCl_4-exposed and the control samples. A ratio of CCl_4/control ≥ 1.5 was used to identify phosphoproteins following CCl_4-exposure, since CCl_4 treatment markedly increased phosphorylation of mitochondrial proteins compared to those of control. The quantified mitochondrial phosphoproteins were further analyzed using MetaCore (GeneGo, St. Joseph, MI, USA) software for molecular toxicity analysis according to the method described previously [28] and for verification of mitochondrial localization of proteins in conjunction with UniProt Knowledgebase (http://www.uniprot.org).

2.4. SDS-PAGE and immunoblot analysis

Mitochondrial fractions were prepared from pooled mouse livers ($n=4$–5/group) from the different treatment groups, as previously described [29,30]. CHAPS-solubilized mitochondrial proteins were dissolved in Laemmli SDS-sample buffer and electrophoresed as per manufacturer's recommendations (Bio-Rad, Hercules, CA) and subjected to immunoblot analysis with the specific antibody to JNK, p-JNK, p-c-Jun, p-Ser-Pro, α-KGDH, ATP5B, NdufS1, or ALDH2, as indicated. The images were visualized by enhanced chemiluminescence detection by following the manufacturer's recommendations (Pierce, Rockford, IL, USA).

2.5. Measurements of liver injury parameters, enzyme activities, and mitochondrial swelling index

Serum alanine aminotransferase (ALT) level from each mouse was determined by using the automated IDEXX Catachem chemistry analyzer system (IDEXX Laboratories, West Brook, ME, USA). The concentration of lipid peroxides as malondialdehyde (MDA)+4-hydroxyalkenal (HAE) (μM) was measured with a commercially available kit (Oxford Biomedical Research, Oxford, MI, USA) by following the manufacturer's protocol. Serum TNFα-levels were determined by using an ELISA assay kit using the manufacturer's protocol (eBioscience, San Diego, CA). Anti-phospho-c-Jun (Ser63) antibody was used to measure JNK activity by immunoblot analysis. Mitochondrial and nuclear fractions from each group were further prepared by subtractive centrifugation, as described [29,30]. The respective marker proteins for cytosol, mitochondria and nuclear fractions were shown to verify relative purity of each fraction (Supplemental Fig. S1). Mitochondrial ALDH2 activity was measured by quantifying the production of NADH at 340 nm, as previously described [31]. One unit of activity was defined as increase in the absorbance at 340 nm per 0.1 mg protein/min multiplied by 1000. NAD^+-dependent ubiquinone-oxidoreductase (mitochondrial complex I) activity was measured by the method previously described [25,32] except that rotenone-containing samples were measured in parallel. Rotenone-sensitive activities were normalized with control sample. Activities of α-ketoglutarate dehydrogenase (α-KGDH) were determined as previously described [33] with a modification where the reaction volumes were reduced to 0.2 mL and 0.1 mg mitochondrial proteins were used for each measurement. One unit of activity was defined as increase in the absorbance at 340 nm per 0.1 mg protein/min multiplied by 1000. Mitochondrial swelling index was determined as described [34]. All activities were measured with a Synergy 2 microplate reader (BioTek, Winooski, VT, USA).

2.6. Immunoprecipitation and immunoblot analysis

Immunoprecipitations of ALDH2, α-KGDH, and NdufS1 (the 75-kDa subunit of complex I) with the specific antibody to each protein were conducted by following the recommended protocol of Dynabeads (Invitrogen-Life Technologies, Grand Island, NY, USA). A separate aliquot of mitochondrial proteins (0.5 mg each) was incubated with 2 μg of antibody-conjugated beads overnight. The immunoprecipitated proteins were dissolved in Laemmli buffer for immunoblot analysis using the specific antibody against each target protein, as indicated [29].

2.7. Intensity data processing and statistical analysis

The intensity of immuno-recognized protein bands such as ALDH2, NdufS1 75-kDa subunit of mitochondrial complex I, α-KGDH, etc on 1-D gels was determined by using a gel digitizing software (UN-SCAN-IT™, Orem, Utah, USA), as previously described [18,25]. All data in this report represent the results from at least three separate experiments, unless stated otherwise. Statistical analyses were performed using the Student's t test and $p < 0.05$ was considered statistically significant. Other methods and materials not described were the same as reported previously [25,28–30] or described in the Supplemental files.

3. Results

3.1. Time-dependent JNK activation and its role in CCl_4-induced liver injury

Our results showed that serum ALT levels remained unchanged until 8 h but markedly increased at 24 h post-CCl_4 injection (Fig. 1A). Consistently, liver histology showed severe pericentral necrosis observed only at 24 h with little liver injury until 8 h post-injection (Fig. 1B). CCl_4-induced liver damage is related to increased lipid peroxidation [5,6] and inflammation as reflected by elevated levels of TNFα [13,35]. However, our data revealed that the levels of lipid peroxide measured by MDA+HAE (Fig. 1C) and serum TNFα (Fig. 1D) remained unchanged up to 8 h, although they were significantly elevated at 24 h post-injection.

Based on rapid JNK activation in CCl_4-exposed rats [17,18,36], we studied the temporal activation of MAPKs in CCl_4-exposed mice by immunoblot analysis. JNK was not activated in corn-oil (control) group, but potently activated (phosphorylated) at 1 and 2 h post-CCl_4 injection (Fig. 2A). Activated p-p38K was detected in control and its levels did not change (i.e., decreased) until 4 h upon CCl_4 exposure. In contrast, the activated p-ERK was detected in control while their levels were increased at 1 or 2 h and returned

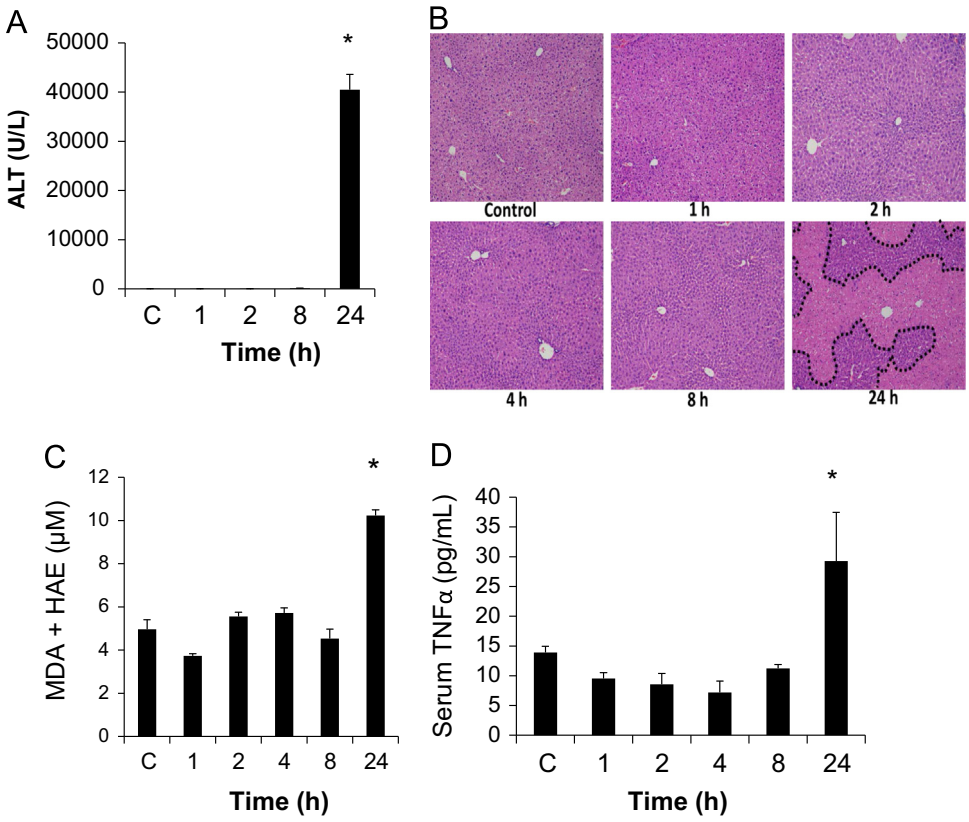

Fig. 1. Time-dependent JNK activation and its role in CCl_4-induced hepatotoxicity in WT mice. (A) Time-dependent changes in the serum ALT levels and (B) typical H&E-stained liver slides are presented for each indicated group (magnification 100 ×). Severe necrotic regions of CCl_4-exposed samples are marked with broken lines in (B). (C) Hepatic levels of MDA+HAE, and (D) serum TNF-alpha levels following CCl_4 exposure are presented. *, Significantly different ($p < 0.05$) from the other groups.

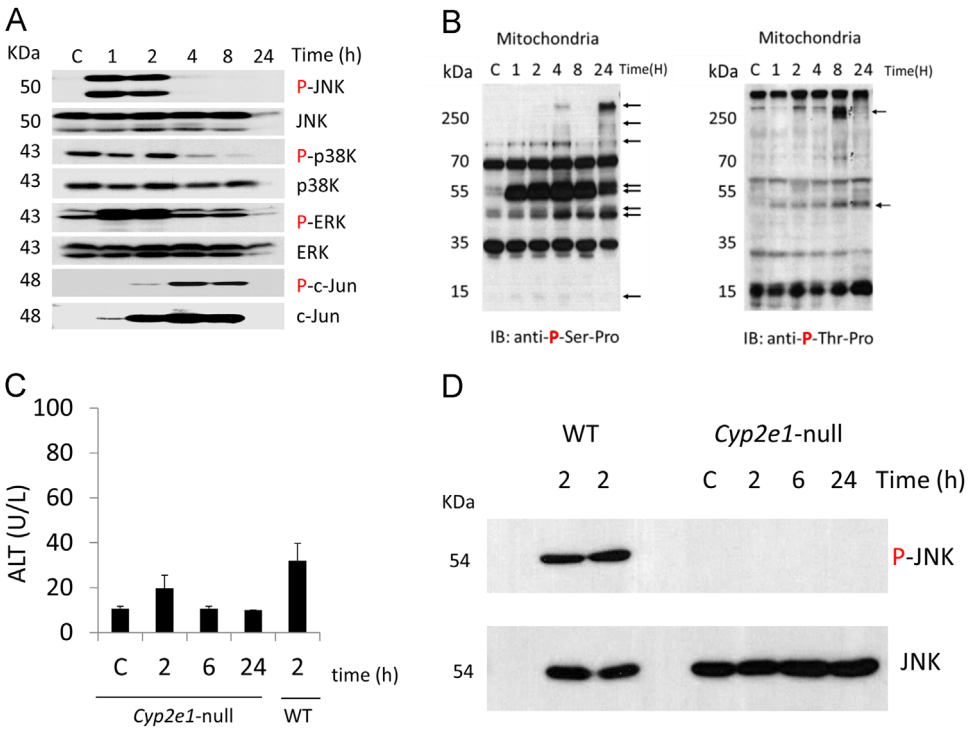

Fig. 2. Time-dependent changes in JNK, phosphorylated mitochondrial proteins and JNK activation in CCl_4–exposed WT or *Cyp2e1*-null mice. (A) Whole cell lysates (50 μg/assay) for indicated samples from WT mice were subjected to immunoblot analysis with the specific anti-p-JNK, anti-p-p38K, anti-p-ERK, their respective non-phospho-proteins, anti-c-Jun, or anti-phospho-c-Jun antibody. (B) Mitochondrial lysates (50 μg/lane) for indicated samples from WT mice were subjected to immunoblot analysis using anti-p-Ser-Pro antibody (left) or anti-p-Thr-Pro antibody (right). Time-dependent changes in the serum ALT levels (C) and JNK activation (D) are presented. Whole cell lysates (50 μg/assay) for indicated samples ($n=4$/each time point) were used to determine JNK activation by immunoblot analysis by using anti-p-JNK antibody (top) and anti-JNK antibody (bottom).

to basal levels at 4 h post-injection (Fig. 2A). The activated phospho-c-Jun was also detected between 2 and 8 h after CCl_4-injection, while c-Jun levels were increased between 1 and 8 h.

3.2. JNK target proteins and role of CYP2E1 in CCl_4-induced JNK activation

The levels of total mitochondrial phosphoproteins, detected by anti-p-Ser-Pro antibody, were markedly increased at 1 h and lasted up to 8 h post-CCl_4 injection (Fig. 2B, left). However, the levels of mitochondrial phosphoproteins, detected by anti-p-Thr-Pro antibody, were very similar between control and CCl_4-exposed samples, except for a few protein bands (Fig. 2B, right). These results suggest that the number and levels of many phosphorylated mitochondrial proteins were increased following CCl_4 exposure, although some phosphoproteins existed in control mice.

We also determined the levels of JNK activation at 2 h and the degrees of acute hepatotoxicity assessed by ALT and histology at 24 h in CCl_4-exposed WT and *Cyp2e1*-null mice. Similar to the earlier reports [9], ALT levels (Fig. 2C) and histological liver damage (data not shown) were very low in CCl_4-exposed *Cyp2e1*-null mice even at 24 h, compared to the corresponding WT mice (Fig. 1A and B, respectively). In addition, the JNK was not activated in *Cyp2e1*-null mice at any time points following CCl_4 exposure, compared to the corresponding WT mice (Fig. 2D). These results suggest that CYP2E1-mediated CCl_4 metabolism is required for JNK activation, which becomes very important in causing acute hepatotoxicity usually observed at later time points [11–14,18].

3.3. Protection of CCl_4-induced liver injury by new selective JNK inhibitors

To further determine the critical role of JNK in mitochondrial dysfunction and liver injury, we evaluated the effects of known chemical inhibitors of JNK on CCl_4-induced JNK activation and translocation of p-JNK to mitochondria at 2 h and hepatotoxicity at 24 h post-CCl_4 injection ($n=4$–5/group). Pretreatment with ATP-competitive JNK inhibitor SP600125 did not prevent CCl_4-induced liver injury determined by serum ALT levels and liver histology (Supplemental Fig. S2A and B, respectively), unlike the earlier reports [12,37]. However, pretreatment with a new specific JNK inhibitor SU3327 [20] significantly protected against CCl_4-induced acute hepatotoxicity assessed by ALT levels (Fig. 3A) and liver histology (Fig. 3B). Pretreatment with another specific JNK inhibitor BI-78D3 [21,22] also showed similar results of protection against CCl_4-induced hepatotoxicity based on the serum ALT levels (Supplemental Fig. S2C).

We further studied the effect of SU3327 on JNK activation and translocation of p-JNK to mitochondria at 2 h post-CCl_4 injection. JNK was potently activated in CCl_4-exposed WT mice (Fig. 3C, top panel, second lane) compared to the control (first lane). SU3327 pretreatment markedly reduced the intensity of active p-JNK in CCl_4-exposed mice (third lane). Consistently, SU3327 pretreatment markedly decreased the amount of active p-JNK translocated to mitochondria (Fig. 3D, top panel, third lane) compared with the corresponding CCl_4-exposed mice (second lane). In contrast, the levels of p-ERK in cytoplasm and mitochondria were unchanged regardless of SU3327 pretreatment (Fig. 3C and D, middle panels, respectively). Consequently, the levels of phosphorylated mitochondrial proteins causally

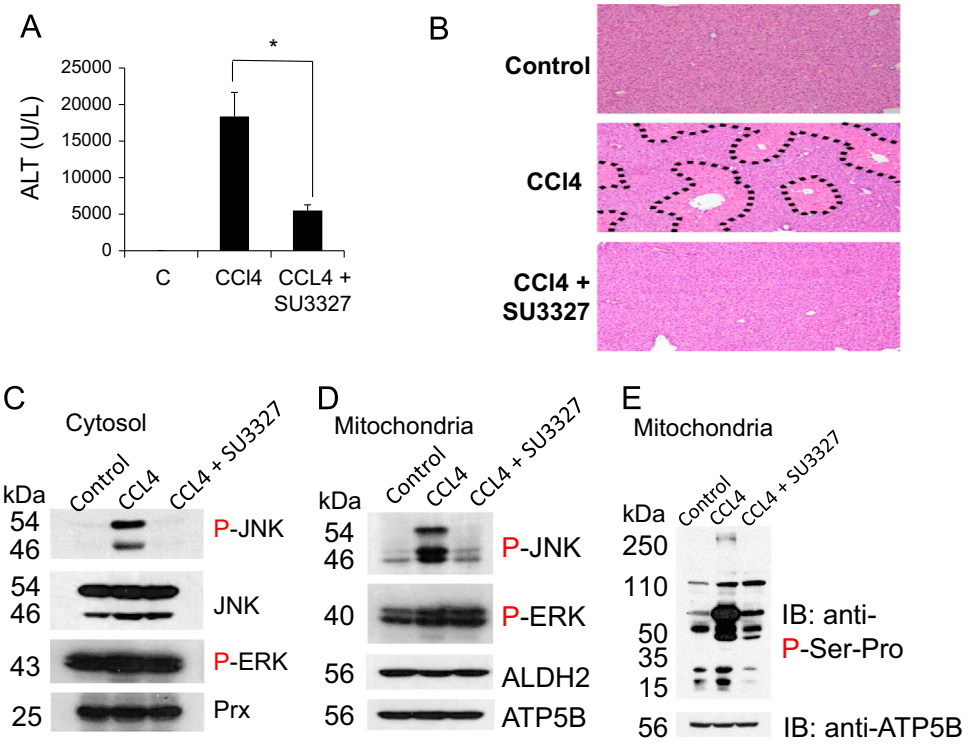

Fig. 3. Pharmacological inhibition of JNK activation alleviates the CCl_4-induced liver injury. (A) Serum ALT levels and (B) H&E-stained liver histology (magnification 100 ×) at 24 h following CCl_4 exposure in WT mice with or without SU3327 pretreatment are presented. *, Significantly different ($p<0.05$) between the two groups. Severe necrotic regions are marked with broken lines. (C) Immunoblot analyses demonstrating relative JNK or ERK activation in the indicated groups treated with CCl_4 for 2 h are presented. Peroxiredoxin (Prx, bottom panel) levels were presented as a loading control. (D) Mitochondrial proteins treated for 2 h (50 μg/lane) were subjected to immunoblot analysis with the specific antibody to phospho-JNK (top), p-ERK (second panel), ALDH2 (third panel), or ATP synthase β-subunit (ATP5B, bottom) used as a loading control. (E) Relative levels of phosphorylated mitochondrial proteins in the indicated samples treated with CCl_4 for 2 h are shown after determining their levels by immunoblot analysis by using anti-p-Ser-Pro antibody (top) or anti-ATP5B as a loading control (bottom).

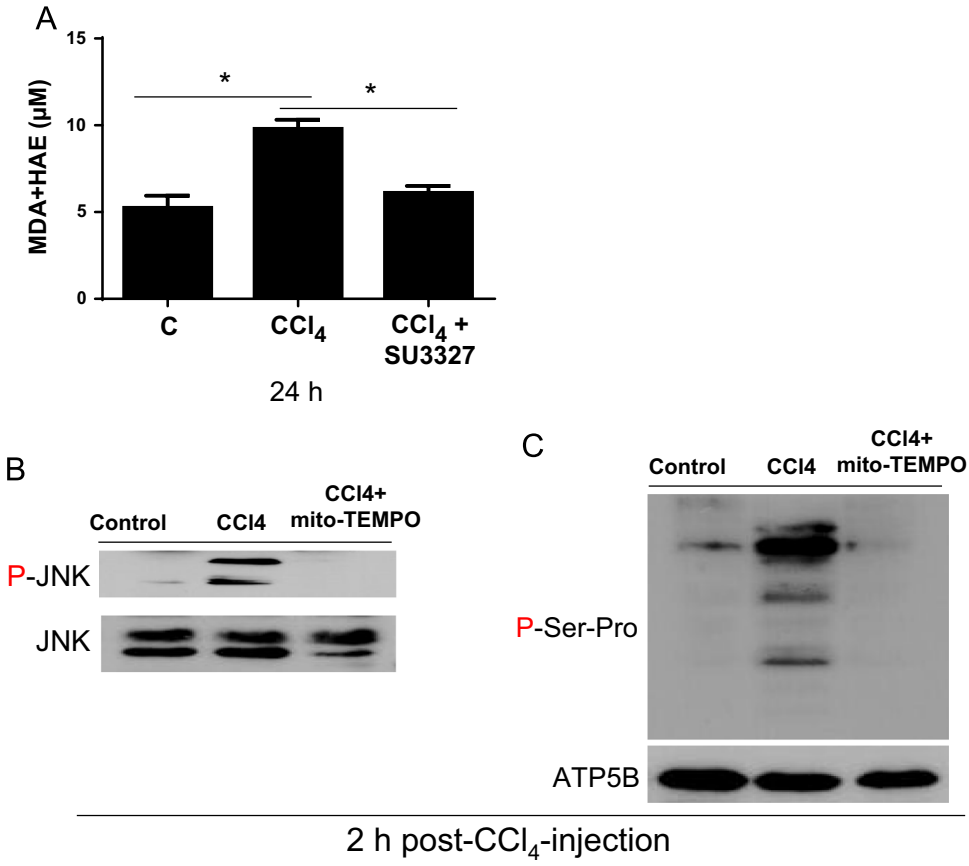

Fig. 4. Effects of SU3327 and mito-TEMPO on the levels of lipid peroxides, p-JNK and mitochondrial protein phosphorylation in CCl_4-exposed mice. (A) The levels of lipid peroxides [MDA+HAE] at 24 h post-CCl_4 injection without or with SU3327 pretreatment are shown. *, Significantly different ($p < 0.05$) between the two groups, as indicated. The Immunoblot results for the levels of (B) active p-JNK and (C) mitochondrial phosphoproteins at 2 h following CCl_4 exposure in WT mice without or with mito-TEMPO pretreatment are presented. Other parameters, including ATP synthase-β subunit (ATP5B, bottom) used as a loading control, are same as the Fig. 3 legend.

correlated with the levels of active p-JNK in CCl_4-exposed mice in the absence or presence of SU3327 pretreatment (Fig. 3E).

We also evaluated the effect of SU3327 on the levels of lipid peroxides as determined by [MDA+HAE]. CCl_4 treatment elevated the levels of [MDA+HAE] (Fig. 4A, second lane) compared to those of vehicle control (first lane) when measured at 24 h, based on the time-dependent increment of lipid peroxides (Fig. 1C). SU3327 pretreatment significantly decreased the levels of lipid peroxides (third lane). We also investigated the effects of the mitochondria-targeted antioxidant mito-TEMPO [23] on the levels of activated p-JNK and phosphorylated mitochondrial proteins. Consistently with the Fig. 2 results, the levels of active p-JNK and mitochondrial phosphoproteins (second lanes of Fig. 4B and C, respectively) were promptly elevated in WT mice exposed to CCl_4 for 2 h, compared to vehicle controls (first lanes). Pretreatment with mito-TEMPO markedly suppressed the levels of p-JNK and phosphoproteins (third lanes of Fig. 4B and C, respectively), compared to those of the mice exposed to CCl_4 alone (middle lanes in Fig. 4B and C, respectively). These results suggest the important role of p-JNK activated at earlier time points in promoting liver injury observed at later times through protein phosphorylation.

3.4. Identification of mitochondrial phosphoproteins

Based on these results with the presence of phosphoproteins in control mice (Figs. 1–4), we purified phosphorylated mitochondrial proteins respectively from vehicle-control and WT mice exposed to CCl_4 for 2 h by using a metal-affinity phosphoprotein purification kit (Qiagen). Subtractive phosphoproteomic analysis of the mass spectral data with a ratio of CCl_4/control groups greater than 1.5-fold revealed that at least 106 mitochondrial proteins were phosphorylated in the CCl_4-exposed samples (Table 1). As summarized in Fig. 5, many proteins, involved in major mitochondrial functions such as energy supply, electron transfer, fatty acid oxidation, anti-oxidant defense, chaperones, amino acid metabolism, etc, were likely phosphorylated by active p-JNK following CCl_4-injection. To systematically evaluate the role of these mitochondrial proteins in any organ toxicities, we performed molecular toxicity and pathology enrichment analysis of these proteins by using MetaCore software. Our analysis revealed that many of these phosphoproteins are highly associated with liver toxicity (Supplemental Fig. S3).

3.5. JNK-mediated phosphorylation and activity changes of the selected mitochondrial proteins

To further evaluate the causal roles of phosphoproteins in hepatotoxicity, we determined the phosphorylation status and activity changes in the three randomly-selected proteins ALDH2, NdufS1 (a 75-kDa subunit of mitochondrial complex I), and α-KGDH in control and CCl_4-exposed mice in the absence or presence of SU3327 pretreatment. We performed immunoprecipitation by using the specific antibody against each target protein. The immunoprecipitated proteins were then subjected to immunoblot analysis with anti-p-Ser-Pro antibody or antibody against each protein. Immunoblot results showed that the mitochondrial levels of ALDH2 remained same regardless of SU3327 pretreatment (Fig. 6A, top panel). ALDH2, un-phosphorylated in the untreated control (middle panel, first lane), was phosphorylated in CCl_4-exposed mice (second lane), despite the similar levels of

Table 1
Summary of phosphorylated mitochondrial proteins in control and CCl4-exposed mouse livers identified by mass-spectral analysis. Subtraction of phosphoproteins in control (CTRL) and CCl4-exposed (EXP) mice was performed as described in the Section 2.3 of Materials and Methods. Only the proteins with the total area ratios greater than 1.5-fold between EXP and CTRL groups are shown.

Accession	Name	Description	Fold (EXP/CTRL)	Normalized Intensity_CTRL (ppm)	Normalized Intensity_EXP (ppm)
IPI00169916.11	Cltc	Clathrin heavy chain 1	137.64	1.11E+01	1.53E+03
IPI00757372.2	Isoc2a	Isochorismatase domain-containing protein 2A, mitochondrial	49.97	1.50E+01	7.48E+02
IPI00120212.1	Ndufa9	NADH dehydrogenase [ubiquinone] 1 alpha subcomplex subunit 9, mito	30.5	1.19E+01	3.64E+02
IPI00319652.2	Gpx1	Glutathione peroxidase 1	30.37	8.33E+01	2.53E+03
IPI00454049.4	Echs1	Enoyl-CoA hydratase, mitochondrial	28.25	2.38E+02	6.72E+03
IPI00468653.4	Pccb	Propionyl-CoA carboxylase beta chain, mitochondrial	21.86	6.24E+01	1.36E+03
IPI00153317.3	Aldh1l1	10-formyltetrahydrofolate dehydrogenase	20.48	3.19E+02	6.52E+03
IPI00122048.2	Atp1a3	Sodium/potassium-transporting ATPase subunit alpha-3	20.16	1.06E+02	2.14E+03
IPI00330523.1	Pcca	Propionyl-CoA carboxylase alpha chain, mitochondrial	18.75	1.42E+02	2.66E+03
IPI00133553.1	Mut	MethyMethylmalonyl-CoA isomerase, involved in the degradation of several amino acids	18.7	3.40E+01	6.36E+02
IPI00311682.5	Atp1a1	Sodium/potassium-transporting ATPase subunit alpha-1	15.7	3.95E+02	6.21E+03
IPI00153660.4	Dlat	Acetyltransferase component of pyruvate dehydrogenase complex	13.88	1.67E+02	2.31E+03
IPI00471246.2	Ivd	Isovaleryl-CoA dehydrogenase, mitochondrial	12.41	1.38E+01	1.71E+02
IPI00420706.4	Lrpprc	Leucine-rich PPR motif-containing protein, mitochondrial	11.07	5.64E+02	6.24E+03
IPI00122549.1	Vdac1	Isoform Pl-VDAC1 of Voltage-dependent anion-selective channel protein 1	10.55	1.87E+01	1.97E+02
IPI00114209.1	Glud1	Glutamate dehydrogenase 1, mitochondrial	9.37	3.57E+03	3.34E+04
IPI00115302.3	Bckdhb	Isoform 2 of 2-oxoisovalerate dehydrogenase subunit beta, mitochondrial	9.32	1.38E+02	1.29E+03
IPI00321718.4	Phb2	Prohibitin-2	9.25	6.36E+01	5.88E+02
IPI00313998.1	Sqrdl	Sulfide:quinone oxidoreductase, mitochondrial	9.12	7.06E+02	6.44E+03
IPI00308882.4	Ndufs1	NADH-ubiquinone oxidoreductase 75 kDa subunit, mitochondrial	9.04	4.34E+02	3.92E+03
IPI00331564.2	Dld	Dihydrolipoyl dehydrogenase	8.88	5.84E+01	5.18E+02
IPI00121440.4	Etfb	Electron transfer flavoprotein subunit beta	8.6	2.91E+02	2.50E+03
IPI00420882.3	Ogdh	Isoform 4 of 2-oxoglutarate dehydrogenase, mitochondrial	8.36	8.06E+00	6.73E+01
IPI00453499.3	Iars2	Isoleucyl-tRNA synthetase, mitochondrial	8.2	4.77E+01	3.91E+02
IPI00130081.2	Pex5	Isoform 2 of Peroxisomal targeting signal 1 receptor	7.42	3.76E+01	2.79E+02
IPI00230138.7	Lyn	Isoform LYN B of Tyrosine-protein kinase Lyn	7.39	1.39E+02	1.03E+03
IPI00469380.3	Aox3	Aldehyde oxidase 1	7.29	2.94E+02	2.14E+03
IPI00331322.3	Mgst1	Microsomal glutathione S-transferase 1	7.06	1.73E+02	1.22E+03
IPI00132799.4	C1qbp	complement component 1 Q subcomponent-binding protein, mitochondrial	6.46	1.42E+02	9.17E+02
IPI00121788.1	Prdx1	Peroxiredoxin	5.91	1.67E+02	9.90E+02
IPI00676071.3	Mosc1	MOSC domain-containing protein 1, mitochondrial	5.77	1.84E+02	1.06E+03
IPI00111908.8	Cps1	Carbamoyl-phosphate synthase [ammonia], mitochondrial	5.63	2.39E+04	1.34E+05
IPI00122862.4	Mthfd1	C-1-tetrahydrofolate synthase, cytoplasmic	5.37	7.54E+02	4.05E+03
IPI00117312.1	Got2	Aspartate aminotransferase, mitochondrial	5.28	1.18E+02	6.23E+02
IPI00126625.1	Acsm1	Isoform 1 of Acyl-coenzyme A synthetase ACSM1, mitochondrial	5.11	2.77E+02	1.41E+03
IPI00109293.1	Lactb	Serine beta-lactamase-like protein LACTB, mitochondrial	5.01	7.79E+02	3.90E+03
IPI00135651.1	Slc25a13	Calcium-binding mitochondrial carrier protein Aralar2	4.73	5.38E+02	2.55E+03
IPI00312174.6	Ptges2	Microsomal prostaglandin E synthase 2	4.71	7.45E+02	3.50E+03
IPI00380320.4	Ldhd	Probable D-lactate dehydrogenase, mitochondrial	4.53	9.83E+01	4.45E+02
IPI00116753.4	Etfa	Electron transfer flavoprotein subunit alpha, mitochondrial	4.31	8.15E+02	3.51E+03
IPI00137194.1	Slc16a1	Monocarboxylate transporter 1	4.26	8.95E+01	3.81E+02
IPI00115117.1	Stoml2	Stomatin-like protein 2	4.12	5.16E+01	2.12E+02
IPI00170363.1	Acsl5	Long-chain-fatty-acid-CoA ligase 5	3.89	6.02E+02	2.34E+03
IPI00319518.4	Lonp1	Lon protease homolog	3.57	1.04E+03	3.72E+03
IPI00115824.1	Nipsnap1	Protein NipSnap homolog 1	3.3	3.86E+02	1.27E+03
IPI00117214.3	Hsdl2	Hydroxysteroid dehydrogenase-like protein 2	3.23	2.22E+02	7.15E+02
IPI00229078.5	Hsd3b4	3-beta-hydroxysteroid dehydrogenase type 4	3.19	2.81E+02	8.96E+02
IPI00120233.1	Gcdh	Glutaryl-CoA dehydrogenase, mitochondrial	2.98	2.61E+02	7.78E+02
IPI00128286.1	Cyp1a1	Cytochrome P450 1A1	2.95	3.17E+02	9.34E+02
IPI00320850.3	Mccc1	Methylcrotonoyl-CoA carboxylase subunit alpha mitochondrial	2.91	4.45E+02	1.30E+03
IPI00122633.3	Acsf2	Acyl-CoA synthetase family member 2, mitochondrial	2.88	9.05E+02	2.61E+03
IPI00114710.3	Pcx	Pyruvate carboxylase, mitochondrial	2.84	3.57E+03	1.01E+04
IPI00133903.1	Hspa9	Heat shock 70 kDa protein 9	2.8	7.43E+03	2.08E+04
IPI00136655.1	Gcat	2-amino-3-ketobutyrate coenzyme A ligase, mitochondrial	2.78	3.48E+02	9.68E+02
IPI00756386.1	Dhtkd1	2-oxoglutarate dehydrogenase E1 component, mitochondrial	2.78	6.06E+02	1.69E+03
IPI00330754.1	Bdh1	3-hydroxybutyrate dehydrogenase	2.71	2.44E+03	6.60E+03
IPI00621548.2	Por	NADPH-cytochrome P450 reductase	2.7	1.46E+03	3.95E+03
IPI00136213.5	Sardh	Sarcosine dehydrogenase, mitochondrial	2.68	7.96E+01	2.14E+02
IPI00379694.4	Hmgcl	hydroxymethylglutaryl-CoA lyase, mitochondrial precursor	2.55	1.44E+02	3.67E+02
IPI00308885.6	Hspd1	Isoform 1 of 60 kDa heat shock protein, mitochondrial	2.54	3.47E+03	8.81E+03
IPI00139301.3	Krt5	Keratin, type II cytoskeletal 5	2.48	8.53E+01	2.12E+02
IPI00461964.3	Aldh6a1	Methylmalonate-semialdehyde dehydrogenase,	2.48	2.23E+03	5.53E+03

Table 1 (*continued*)

Accession	Name	Description	Fold (EXP/CTRL)	Normalized Intensity_CTRL (ppm)	Normalized Intensity_EXP (ppm)
		mitochondrial			
IPI00111218.1	Aldh2	Aldehyde dehydrogenase, mitochondrial	2.38	2.30E+03	5.49E+03
IPI00223092.5	Hadha	Trifunctional enzyme subunit alpha, mitochondrial	2.37	1.72E+03	4.06E+03
IPI00270326.1	Psmc2	26S protease regulatory subunit 7	2.37	3.80E+01	8.99E+01
IPI00226140.5	Maob	Amine oxidase [flavin-containing] B	2.36	7.37E+02	1.74E+03
IPI00331436.4	Lap3	Isoform 1 of Cytosol aminopeptidase	2.29	5.99E+01	1.37E+02
IPI00119114.2	Acadl	Long-chain specific acyl-CoA dehydrogenase, mitochondrial	2.26	8.94E+02	2.02E+03
IPI00116603.1	Otc	Ornithine carbamoyltransferase, mitochondrial	2.23	6.57E+02	1.47E+03
IPI00132042.1	Pdhb	Pyruvate dehydrogenase E1-beta subunit, mitochondrial	2.23	1.32E+03	2.96E+03
IPI00113052.1	Tsfm	Elongation factor Ts, mitochondrial	2.22	1.09E+02	2.41E+02
IPI00118384.1	Ywhae	14-3-3 protein epsilon	2.21	7.79E+02	1.72E+03
IPI00331555.2	Bckdha	2-oxoisovalerate dehydrogenase subunit alpha, mitochondrial	2.17	8.44E+03	1.83E+04
IPI00322610.5	Coasy	Bifunctional coenzyme A synthase	2.15	1.11E+02	2.39E+02
IPI00132762.1	Trap1	Heat shock protein 75 kDa, mitochondrial	2.14	2.70E+03	5.77E+03
IPI00322760.7	Prodh	Proline dehydrogenase, mitochondrial	2.14	2.35E+03	5.03E+03
IPI00112549.1	Acsl1	Long-chain specific acyl-CoA synthetase 1	2.09	4.20E+03	8.78E+03
IPI00323357.3	Hspa8	Heat shock cognate 71 kDa protein	2.07	2.55E+03	5.27E+03
IPI00134746.5	Ass1	Argininosuccinate synthase	2.02	1.47E+03	2.96E+03
IPI00121105.2	Hadh	Hydroxyacyl-coenzyme A dehydrogenase, mitochondrial	2.01	1.53E+02	3.06E+02
IPI00131445.2	Dnm2	Isoform 1 of Dynamin-2 GTPase	1.95	1.89E+02	3.70E+02
IPI00678532.3	Fam82a2	Regulator of microtubule dynamics protein 3	1.92	1.68E+02	3.22E+02
IPI00130535.1	Dbt	Lipoamide acyltransferase of branched-chain alpha-keto acid dehydrogenase complex	1.9	1.53E+03	2.90E+03
IPI00130804.1	Ech1	Delta(3,5)-Delta(2,4)-dienoyl-CoA isomerase, mitochondrial	1.88	3.75E+02	7.07E+02
IPI00119203.4	Acadvl	Very long-chain specific acyl-CoA dehydrogenase, mitochondrial	1.87	3.41E+03	6.36E+03
IPI00122075.1	Mavs	Mitochondrial antiviral-signaling protein	1.86	4.93E+02	9.15E+02
IPI00134809.2	Dlst	Succinyltransferase component of 2-oxoglutarate dehydrogenase complex	1.85	4.85E+02	8.97E+02
IPI00119808.1	Clpx	ATP-dependent ClpX-like protease, mitochondrial	1.84	1.06E+03	1.95E+03
IPI00169862.1	Coq9	Ubiquinone biosynthesis protein COQ9, mitochondrial	1.78	9.68E+02	1.73E+03
IPI00127841.3	Slc25a5	ADP/ATP translocase 2	1.77	7.18E+02	1.27E+03
IPI00131177.1	Letm1	LETM1 and EF-hand domain-containing protein 1, mitochondrial	1.75	1.26E+03	2.20E+03
IPI00408961.3	Haao	3-hydroxyanthranilate 3,4-dioxygenase	1.73	1.06E+02	1.83E+02
IPI00387491.1	Aass	Alpha-aminoadipic semialdehyde synthase, mitochondrial	1.7	5.45E+02	9.27E+02
IPI00120123.1	Dmgdh	Dimethylglycine dehydrogenase, mitochondrial	1.7	1.07E+03	1.82E+03
IPI00459487.3	Suclg2	Isoform 1 of Succinyl-CoA ligase subunit beta, mitochondrial	1.69	1.61E+03	2.72E+03
IPI00135231.2	Idh1	Isocitrate dehydrogenase	1.66	5.24E+02	8.70E+02
IPI00317074.3	Slc25a10	Mitochondrial dicarboxylate carrier	1.61	1.89E+02	3.05E+02
IPI00115564.5	Slc25a4	ADP/ATP translocase 1	1.6	7.06E+02	1.13E+03
IPI00116498.1	Ywhaz	14-3-3 protein zeta/delta	1.58	6.25E+02	9.89E+02
IPI00127625.1	Hmgcl	Hydroxymethylglutaryl-CoA lyase, mitochondrial	1.56	8.03E+02	1.25E+03
IPI00113886.1	Lmnb2	Lamin B2 isoform	1.55	1.13E+03	1.76E+03
IPI00110684.1	Ppa1	inorganic pyrophosphatase	1.55	3.81E+01	5.92E+01
IPI00130280.1	Atp5a1	ATP synthase subunit alpha, mitochondrial	1.53	1.51E+04	2.32E+04
IPI00230108.6	Pdia3	Protein disulfide-isomerase A3	1.53	4.26E+03	6.52E+03
IPI00113869.1	Bsg	Isoform 2 of Basigin	1.53	1.47E+02	2.24E+02
IPI00119842.1	Acadsb	Short/branched chain acyl-CoA dehydrogenase, mitochondrial	1.53	8.58E+01	1.32E+02

immunoprecipitated ALDH2 protein for each lane (bottom panel). However, the intensity of phosphorylated ALDH2 was markedly reduced upon SU3327 pretreatment (middle panel, third lane), suggesting reversible phosphorylation of ALDH2, depending on the JNK activity. Consistently, the ALDH2 activity in the mitochondrial extracts was significantly suppressed in WT mice exposed to CCl_4 for 2 h compared to the control group, but its suppressed activity was restored in SU3327-pretreated mice (Fig. 6B).

In addition, the levels of NdufS1 were similar in differently-treated mice regardless of SU3327 pretreatment (Fig. 6C, top panel). NdufS1 phosphorylation was markedly increased in CCl_4-exposed WT mice (middle panel, second lane), compared to the untreated control (first lane). The intensity of the phosphorylated protein band was markedly reduced in SU3327-pretreated mice (third lane). Consistently, the mitochondrial complex I activity was significantly decreased in CCl_4-exposed WT mice compared with those of control (Fig. 6D). Furthermore, the decreased activity was restored in the SU3327-pretreated group.

Similar patterns of reversible phosphorylation (Fig. 6E) and activity change (Fig. 6F) in α-KGDH were observed in CCl_4-exposed mice in the absence or presence of SU3327. These results (Fig. 6) not only substantiate the presence of phosphoproteins determined by mass spectrometry but also support that JNK-mediated phosphorylation of certain mitochondrial proteins is responsible for the suppressed activities at 2 h, contributing to CCl_4-induced mitochondrial dysfunction and liver injury observed at later time points (e.g., at 24 h as shown in Fig. 1).

Activated p-JNK can phosphorylate pro-apoptotic Bax to promote mitochondrial permeability transition (MPT) change and cell damage [15,38]. Our results showed that time-dependent mitochondrial translocation of Bax and subsequent release of cytochrome C were maximal at 2 h post-CCl_4 injection (Fig. 7A). However, these events were significantly blocked by the SU3327 treatment (Fig. 7B). Consistently, CCl_4 exposure significantly increased time-dependent mitochondrial swelling (Fig. 7C), which was significantly prevented by SU3327 pretreatment (Fig. 7D),

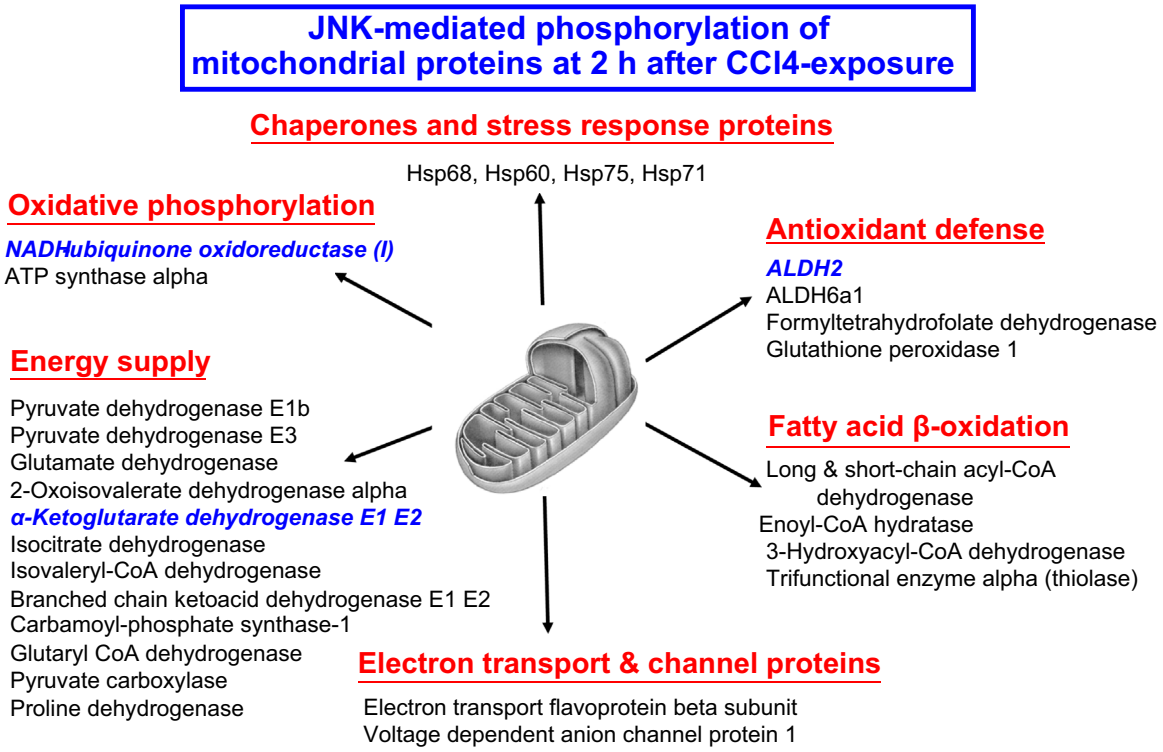

Fig. 5. Summary of phosphorylated mitochondrial proteins in WT mice exposed to CCl_4 for 2 h. Various functions of mitochondrial proteins that were phosphorylated in CCl_4-exposed mouse liver and identified by mass spectrometry are summarized. The activities of the three proteins marked in *blue and bold characters* were suppressed in CCl_4-exposed mice compared to the corresponding vehicle-controls. (For interpretation of the references to color in this figure legend, the reader is referred to the web version of this article.)

supporting JNK-dependent MPT change and mitochondrial dysfunction, prior to hepatotoxicity.

4. Discussion

Molecular mechanisms of acute liver injury caused by many compounds including FDA-approved drugs such as APAP and troglitazone, an anti-diabetic agent, have been actively studied because of severe mitochondrial dysfunction and hepatotoxicity [1–4,39–43]. Many abused substances including cocaine and amphetamine derivatives are also known to cause mitochondrial dysfunction and acute hepatotoxicity [44,45] especially in people who drink alcohol [44]. From the experimental models, many different mechanisms have been proposed to explain the acute hepatotoxicity. These mechanisms include: production of reactive metabolites and protein adducts, increased oxidative/nitrative stress, protein modifications and subsequent mitochondrial dysfunction, lipid peroxidation, inflammation through activation of innate immune responses, toxic ceramide production, activation of the cell death pathways, suppression of the cell proliferation/survival pathway, etc. [45–48]. In general, all these mechanisms work together toward tissue injury, as recently discussed [47,48].

Activation of JNK alone or in combination with p38K is responsible for promoting cell death [10,11]. Other laboratories and we reported the critical role of JNK activation in drug-induced acute hepatotoxicity [12–15,37–39] and ischemia-reperfusion injury [16]. Although JNK was the main MAPK activated by CCl_4 exposure [17,36] and in our current study (Figs. 1 and 3), another report suggested that activated JNK did not seem to be critical in CCl_4-mediated liver injury through evaluation with the ATP-competitive JNK inhibitor SP600125 and the JNK peptide inhibitor-1 (D-JNKI-1), which interferes with the interaction between JNK and its substrates [13]. The negative role of JNK in CCl_4-related hepatotoxicity [13] could result from: (1) the additional activity of SP600125 and its non-specific inhibition of other protein kinases [49–52]; (2) potential compensatory mechanisms between the JNK1 and JNK2 isoforms in the liver; (3) potential toxicity of SP600125 by itself in some cases [53]; (4) a relatively high dosage of CCl_4 in a different mouse strain used for the previous study [13] compared to this current study; and (5) no usage of other selective JNK inhibitors such as SU3327 and BI-78D3 [20–22]. Furthermore, to our knowledge, the identities and functional roles of mitochondrial phosphoprotein targets of active p-JNK have never been studied systematically. Therefore, in the current study, we aimed to re-evaluate the role of JNK in promoting liver injury caused by CCl_4, as a model of acute hepatotoxicity, by carefully studying the time-dependent JNK activation and the levels of its mitochondrial phosphoprotein targets, lipid peroxides and liver injury with two newly-developed highly-specific JNK inhibitors SU33327 [20] and BI-78D3 [21,22]. Since APAP can cause liver injury by promoting protein nitration [54,55] in addition to JNK-mediated protein phosphorylation [12,13], we intentionally chose to use CCl_4 in this study to re-investigate the roles of JNK activation and JNK-mediated protein phosphorylation at early time points prior to mitochondrial dysfunction and acute liver injury, based on the relatively selective activation of JNK by CCl_4 [17,36]. We now provide evidence that p-JNK activated at earlier time points plays a pivotal role in promoting CCl_4-induced mitochondrial dysfunction and hepatotoxicity through phosphorylation of many mitochondrial proteins and inactivation of their functions. However, these events were markedly reduced in the presence of the two new JNK-specific inhibitors SU3327 (Figs. 3, 4 and 6) and BI-78D3 (not shown). Furthermore, neither JNK activation nor hepatotoxicity was observed in CCl_4-exposed *Cyp2e1*-null mice despite the same treatment of CCl_4 (Fig. 2). We also showed that prompt JNK activation, translocation of active p-JNK to mitochondria, and protein phosphorylation likely represent the

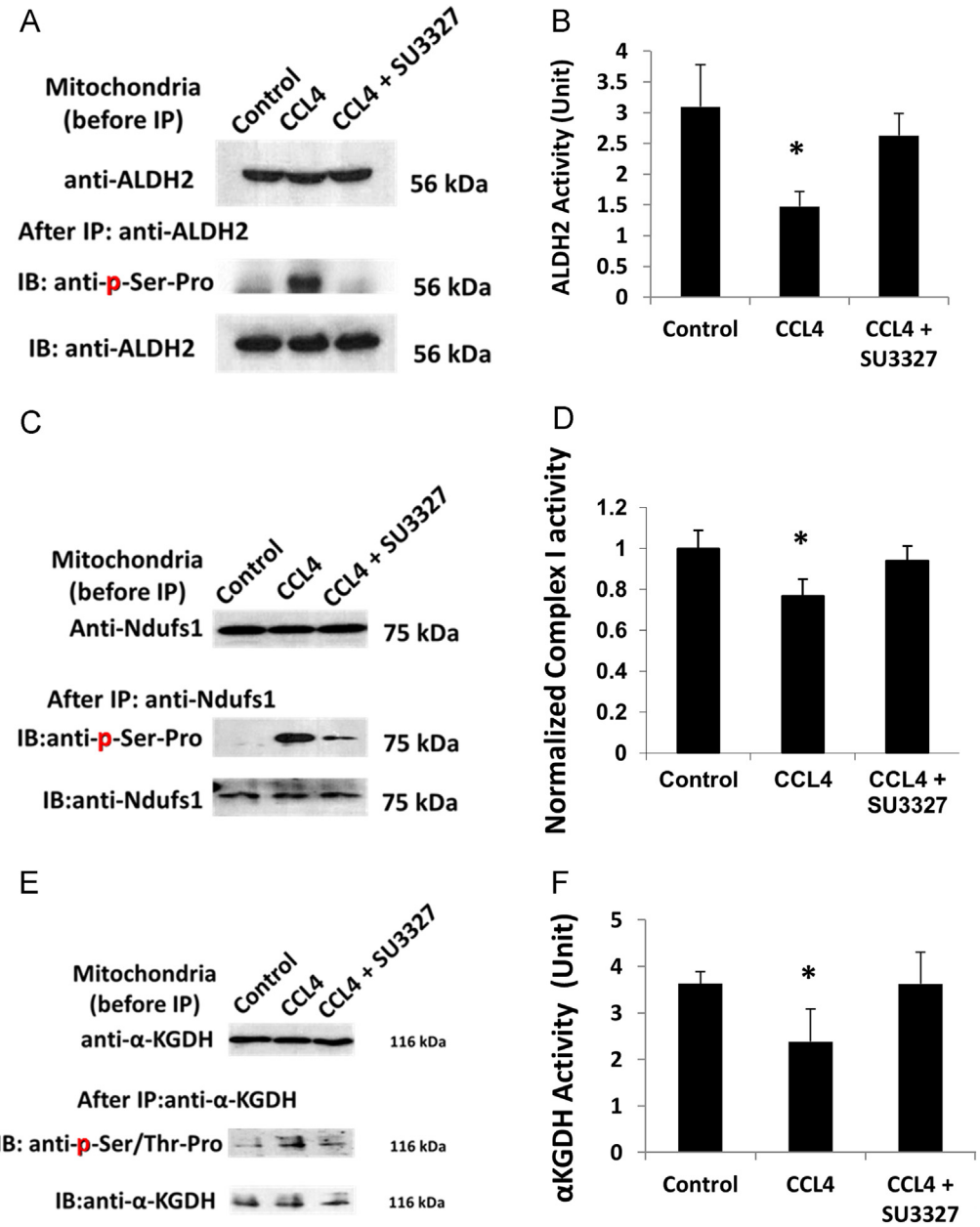

Fig. 6. Selected mitochondrial proteins are phosphorylated and their activities suppressed by p-JNK. (A) The level of mitochondrial ALDH2 in control and CCl_4-exposed WT mice in the absence or presence of SU3327 pretreatment was determined by immunoblot analysis (top panel). Mitochondrial proteins (0.5 mg/analysis) from vehicle-control and mice exposed to CCl_4 for 2 h in the absence or presence of SU3327 were immunoprecipitated with anti-ALDH2 antibody and then subjected to immunoblot analysis with anti-p-Ser-Pro antibody (middle) or anti-ALDH2 antibody (bottom). (B) ALDH2 activity in mitochondrial extracts (0.1 mg protein/assay) for the indicated groups with or without SU3327 pretreatment was determined. Additional analyses were conducted on NdufS1 (complex I) (C, D) and α-KGDH (E, F), as indicated. *, Significantly different ($p < 0.05$) from the other groups.

critical events in CCl_4-mediated hepatotoxicity than lipid peroxidation [5,6], nitrative stress [54,55], and TNFα-associated inflammation, as previously suggested [13,35], since these latter factors were elevated only at 24 h post-CCl_4 exposure (Fig. 1 and data not shown). Based on these time-dependent observations, we believe that lipid peroxidation and inflammation likely reflect the consequences rather than the causes of hepatotoxicity. Furthermore, the results with *Cyp2e1*-null mice (Fig. 2) and mito-TEMPO (Fig. 4) indicate that CYP2E1-mediated CCl_4 metabolism induces oxidative stress, which can rapidly activate JNK (Fig. 2) resulting from inhibition of MAPK phosphatases through oxidative modifications of their active site Cys and other critical Cys residues, as recently reviewed [48]. Activated p-JNK then translocates to mitochondria and phosphorylates many proteins including mitochondrial complex I, resulting in suppression of the mitochondrial electron transport chain, and thus markedly elevating oxidative stress, which ultimately contributes to mitochondrial dysfunction and hepatotoxicity with increased lipid peroxidation observed at later time points.

In addition, JNK was reported to promote cell death through phosphorylating Bax, which contributes to mitochondrial permeability transition (MPT) change (swelling) and apoptosis [15, 39]. It is well-established that activated p-JNK translocates to mitochondria upon exposure to various toxic stimulants such as staurosporine, ionizing radiation, UV [15] and anisomycin [56]. Hanawa et al. reported that activated p-JNK was translocated to mitochondria to induce MPT and inhibit mitochondrial respiration, leading to acute hepatocyte injury in APAP-exposed mice [39]. Our previous report also showed that p-JNK

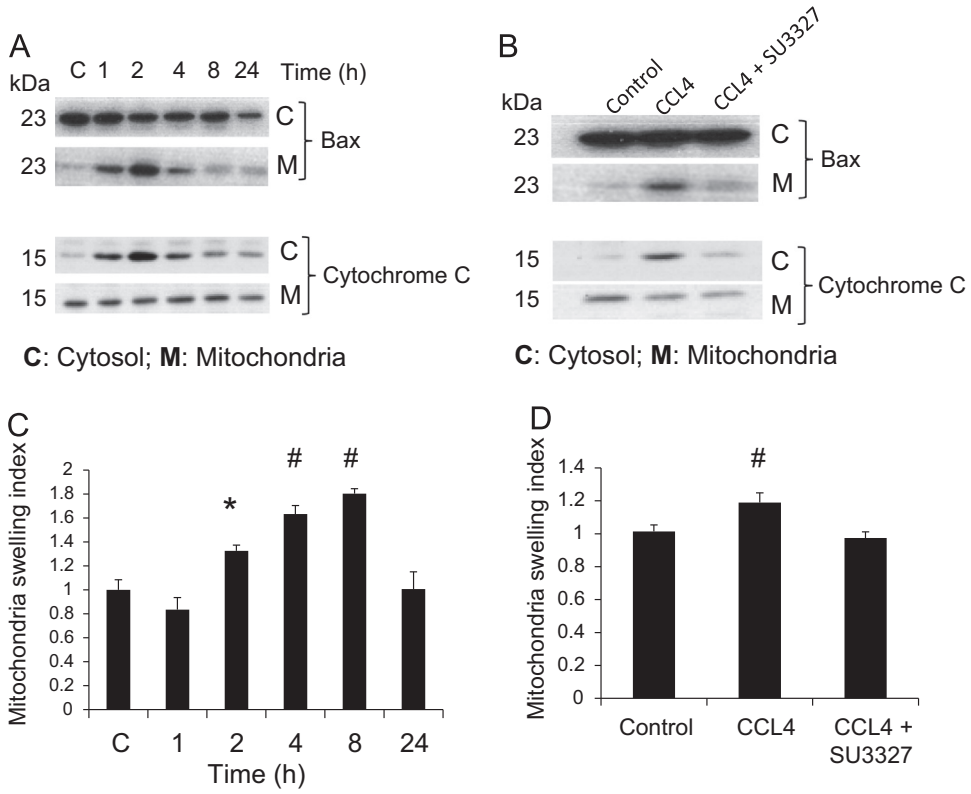

Fig. 7. Time-dependent changes in Bax, cytochrome C, and mitochondrial swelling in CCl_4-exposed mice. WT mice were exposed to CCl_4 alone for indicated time points (A, C) or only for 2 h in the absence or presence of SU3327 pretreatment (B, D) before tissue collection. (A, B) Time-dependent changes in the cytosolic or mitochondrial amounts of Bax and cytochrome C are presented after determining their levels by immunoblot analysis using the specific antibody to each protein. (C, D) Time-dependent changes in the mitochondrial swelling index for the indicated samples are presented. *,#, Significantly different ($p < 0.05$) from the other groups.

was activated in CCl_4-exposed rats and translocated to mitochondria where it could phosphorylate mitochondrial ALDH2 [18]. However, to our knowledge, the JNK-target proteins in mitochondria are poorly understood, although PDH E1α and β subunits, Hsp60 and ATP synthase were phosphorylated by active p-JNK in an *in vitro* system [19]. Therefore, another aim of this study was to systematically identify mitochondrial target proteins that are phosphorylated by p-JNK and study their contributing roles in CCl_4-related mitochondrial dysfunction and hepatotoxicity. By using mass-spectral analysis of the affinity-purified phosphoproteins (with more than 2 different peptides identified by mass spectrometry) and using subtraction phospho-proteomics with the ratio of CCl_4/control greater than 1.5, we found that at least 106 mitochondrial proteins, including ALDH2, NAD^+-ubiquinone-dehydrogenase, α-KGDH, etc were likely phosphorylated (Table 1). Although our result also confirmed the small list of JNK-target phosphoproteins from the *in vitro* experiment [19], we believe that the actual number of JNK-target proteins in mitochondria could be a lot more than what we identified in this study, since the JNK-target proteins existing in small amounts, such as Bax [15] and Sab [57,58], may not be detected due to the detection limit of our mass-spectral analysis. Despite this disadvantage, by using immunoprecipitation followed by immunoblot with anti-phospho-Ser-Pro antibody, we confirmed JNK-mediated phosphorylation of the three selected target proteins in CCl_4-exposed mice. Furthermore, we demonstrate the functional roles of some of the phosphoproteins since the suppressed activities of these proteins were restored by JNK inhibitor SU3327 pretreatment. We expect that the activities of other phosphorylated proteins in CCl_4-exposed mice could be also modulated through JNK-mediated phosphorylation.

The mechanisms of CCl_4-induced mitochondrial dysfunction have not been fully understood despite previous efforts [5,6 and references within]. Based on our results of the suppressed activities of phosphorylated mitochondrial proteins despite similar protein levels (Fig. 6), post-translational modifications of mitochondrial proteins by p-JNK activated at earlier time points (Fig. 2) are at least partially responsible for CCl_4-induced mitochondrial dysfunction prior to hepatotoxicity. Our results showed that α-KGDH and complex I, involved in cell energy supply, were suppressed in CCl_4-exposed tissues compared to control. ALDH2, involved in anti-oxidant defense, was also suppressed following CCl4 exposure. Since JNK activation and phosphorylation occurred earlier (e.g., 1 or 2 h) and led to inactivation of ALDH2, complex I, and α-KGDH, their suppression was likely to promote mitochondrial dysfunction, contributing to increased MPT [38], and eventually liver injury observed at 24 h post-injection. Although we have not tested many other phosphoproteins, it is likely that the activities of some of the phosphorylated mitochondrial proteins may be modulated in a JNK-dependent manner. Thus, our current study provides a novel mechanism for CCl_4-induced mitochondrial dysfunction and hepatotoxicity through JNK-mediated phosphorylation of many mitochondrial proteins

Although we have purified and identified phosphorylated mitochondrial proteins by mass-spectral analysis, we do not know specific phosphorylation sites yet. The canonical JNK binding motif sequence is: R/K_{2-3}-X_{1-6}-L/I-X-L/I [59]. Based on the comparative sequence analysis between mitochondrial ALDH2 and cytosolic ALDH1, we reported that ^{463}Ser-Pro of ALDH2 could be the prime site of JNK-mediated phosphorylation [18]. We also observed that 75 kDa-subunit NdufS1 subunit of complex I was phosphorylated after CCl_4 exposure. This protein also contains one putative JNK binding site at ^{515}K-R-N-P-P-K-M-L-F-L, and four potential phosphorylation sites (Ser^{411}-Pro, Ser^{425}-Pro, Thr^{588}-Pro, Ser^{627}-Pro) by active p-JNK. Sequence analysis revealed that α-KGDH contains one canonical JNK binding motif at ^{376}K-K-V-M-S-I-L-L, and eight

potential phosphorylation sites (Ser^{55}-Pro, Thr^{215}-Pro, Ser^{433}-Pro, Ser^{562}-Pro, Ser^{711}-Pro, Thr^{809}-Pro, Thr^{833}-Pro, Ser^{909}-Pro) by p-JNK. However, the exact sites of phosphorylation in these proteins remain to be established.

In conclusion, by studying temporal changes in JNK activation, lipid peroxidation, pro-inflammatory TNF-α levels and histological liver damage following CCl_4 administration, we demonstrated the critical role of JNK activation and subsequent protein phosphorylation in chemical-induced mitochondrial dysfunction and acute hepatotoxicity. We have affinity-purified phosphorylated mitochondrial proteins from CCl_4-exposed mouse liver and control tissues and determined their identities by mass-spectral analysis. Our results revealed that many mitochondrial proteins were phosphorylated by p-JNK and that their cellular functions could be altered, contributing to mitochondrial dysfunction and hepatotoxicity. By using two new JNK-specific inhibitors SU3327 and BI-78D3, which potently blocked JNK without affecting ERK activity, we also showed that the activities of the selected phosphorylated mitochondrial proteins and hepatotoxicity were reversibly modulated in a JNK-dependent manner, suggesting a causal relationship between JNK-mediated phosphorylation of mitochondrial proteins and their functions. These data demonstrate for the first time an important role of JNK-mediated phosphorylation of many mitochondrial proteins in promoting chemical-induced mitochondrial dysfunction and acute liver injury.

Disclosure

All authors do not have conflict of interest.

Acknowledgments

This study was supported by the Intramural Research Program of National Institute of Alcohol Abuse and Alcoholism (NIAAA) and in part with funds from the Intramural Fund of National Center for Toxicological Research, U.S. Food and Drug Administration (NCTR/FDA). The views presented in this article do not necessarily reflect those of the U.S. Food and Drug Administration. The authors are also grateful to Drs. Youngshim Choi and Klaus Gawrisch for the excellent technical help and support for this study, respectively.

Appendix A. Supplementary material

Supplementary data associated with this article can be found in the online version at http://dx.doi.org/10.1016/j.redox.2015.09.040.

References

[1] W.M. Lee, Acetaminophen and the U.S. acute liver failure study group: lowering the risks of hepatic failure, Hepatology 40 (2004) 6–9.
[2] R.T. Chung, R.T. Stravitz, R.J. Fontana, F.V. Schiodt, W.Z. Mehal, K.R. Reddy, W. M. Lee, Pathogenesis of liver injury in acute liver failure, Gastroenterology 143 (2012) e1–e7.
[3] C.J. McClain, J.P. Kromhout, F.J. Peterson, J.L. Holtzman, Potentiation of acetaminophen hepatotoxicity by alcohol, JAMA 244 (1980) 251–253.
[4] L.B. Seeff, B.A. Cuccherini, H.J. Zimmerman, E. Adler, S.B. Benjamin, Acetaminophen hepatotoxicity in alcoholics, Ann. Int. Med. 104 (1986) 399–404.
[5] R.O. Recknagel, E. Glende Jr., J.A. Dolak, R.L. Waller, Mechanisms of carbon tetrachloride toxicity, Pharmacol. Ther. 43 (1989) 139–154.
[6] L. Weber, M. Boll, A. Stampfl, Hepatotoxicity and mechanism of action of haloalkanes: carbon tetrachloride as a toxicological model, Crit. Rev. Toxicol. 33 (2003) 105–136.
[7] D.P. Hartley, D.J. Kroll, D.R. Petersen, Prooxidant-initiated lipid peroxidation in isolated rat hepatocytes: detection of 4-hydroxynonenal- and malondialdehyde-protein adducts, Chem. Res. Toxicol. 10 (1997) 895–905.
[8] P. Muriel, Nitric oxide protection of rat liver from lipid peroxidation, collagen accumulation, and liver damage induced by carbon tetrachloride, Biochem. Pharmacol. 56 (1998) 773–779.
[9] F.W.Y. Wong, W.Y. Chan, Lee SST, Resistance to carbon tetrachloride-induced hepatotoxicity in mice which lack CYP2E1 expression, Toxicol. Appl. Pharmacol. 153 (1998) 109–118.
[10] Z. Xia, M. Dickens, J. Raingeaud, R.J. Davis, M.E. Greenberg, Opposing effects of ERK and JNK-p38 MAP kinases on apoptosis, Science 270 (1995) 1326–1331.
[11] E. Seki, D.A. Brenner, M. Karin, A liver full of JNK: signaling in regulation of cell function and disease pathogenesis, and clinical approaches, Gastroenterology 143 (2012) 307–320.
[12] B.K. Gunawan, Z.X. Liu, D. Han, N. Hanawa, W.A. Gaarde, N. Kaplowitz, c-Jun N-terminal kinase plays a major role in murine acetaminophen hepatotoxicity, Gastroenterology 131 (2006) 165–178.
[13] N.C. Henderson, K.J. Pollock, J. Frew, A.C. Mackinnon, R.A. Flavell, R.J. Davis, T. Sethi, K.J. Simpson, Critical role of c-jun (NH2) terminal kinase in paracetamol-induced acute liver failure, Gut 56 (2007) 982–990.
[14] M.A. Bae, J.E. Pie, B.J. Song, Acetaminophen induces apoptosis of C6 glioma cells by activating the c-Jun NH2-terminal protein kinase-related cell death pathway, Mol. Pharmacol. 60 (2001) 847–856.
[15] B.J. Kim, S.W. Ryu, B.J. Song, JNK- and p38 kinase-mediated phosphorylation of Bax leads to its activation and mitochondrial translocation and to apoptosis of human hepatoma HepG2 cells, J. Biol. Chem. 281 (2006) 21256–21265.
[16] T. Uehara, B. Bennett, S.T. Sakata, Y. Satoh, G.K. Bilter, J.K. Westwick, D. A. Brenner, JNK mediates hepatic ischemia reperfusion injury, J. Hepatol. 42 (2005) 850–859.
[17] K.G. Mendelson, L.R. Contois, S.G. Tevosian, R.J. Davis, K.E. Paulson, Independent regulation of JNK/p38 mitogen-activated protein kinases by metabolic oxidative stress in the liver, Proc. Nat. Acad. Sci. USA 93 (1996) 12908–12913.
[18] K.H. Moon, Y.M. Lee, B.J. Song, Inhibition of hepatic mitochondrial aldehyde dehydrogenase by carbon tetrachloride through JNK-mediated phosphorylation, Free Radic. Biol. Med. 48 (2010) 391–398.
[19] H. Schroeter, C.S. Boyd, R. Ahmed, J.P. Spencer, R.F. Duncan, C. Rice-Evans, E. Cadenas, c-Jun N-terminal kinase (JNK)-mediated modulation of brain mitochondria function: new target proteins for JNK signalling in mitochondrion-dependent apoptosis, Biochem. J. 372 (2003) 359–369.
[20] S.K. De, J.L. Stebbins, L.H. Chen, M. Riel-Mehan, T. Machleidt, R. Dahl, H. Yuan, A. Emdadi, E. Barile, V. Chen, R. Murphy, M. Pellecchia, Design, synthesis, and structure– activity relationship of substrate competitive, selective, and in vivo active triazole and thiadiazole inhibitors of the c-Jun N-terminal kinase, J. Med. Chem. 52 (2009) 1943–1952.
[21] J.L. Stebbins, S.K. De, T. Machleidt, B. Becattini, J. Vazquez, C. Kuntzen, L. H. Chen, J.F. Cellitti, M. Riel-Mehan, A. Emdadi, G. Solinas, M. Karin, M. Pellecchia, Identification of a new JNK inhibitor targeting the JNK–JIP interaction site, Proc. Nat. Acad. Sci. USA 105 (2008) 16809–16813.
[22] D.W. Borhani, Covalent JNK inhibitors? Proc. Nat. Acad. Sci. USA 106 (2009) E18.
[23] A. Weidinger, A. Müllebner, J. Paier-Pourani, A. Banerjee, I. Miller, L. Lauterböck, J.C. Duvigneau, V.P. Skulachev, H. Redl, A.V. Kozlov, Vicious inducible nitric oxide synthase-mitochondrial reactive oxygen species cycle accelerates inflammatory response and causes liver injury in rats, Antioxid. Redox Signal. 22 (2015) 572–586.
[24] M.A. Abdelmegeed, A. Banerjee, S. Jang, S.H. Yoo, J.W. Yun, F.J. Gonzalez, A. Keshavarzian, B.J. Song, CYP2E1 potentiates binge alcohol-induced gut leakiness, steatohepatitis, and apoptosis, Free Radic. Biol. Med. 65 (2013) 1238–1245.
[25] K.H. Moon, V.V. Upreti, L.R. Yu, I.J. Lee, X. Ye, N.D. Eddington, T.D. Veenstra, B. J. Song, Mechanism of 3,4-methylenedioxymethamphetamine (MDMA, ecstasy)-mediated mitochondrial dysfunction in rat liver, Proteomics 8 (2008) 3906–3918.
[26] D.H. Lundgren, S.I. Hwang, L. Wu, D.K. Han, Role of spectral counting in quantitative proteomics, Expert Rev. Proteom. 7 (2010) 39–53.
[27] Q. Jin, L.R. Yu, L. Wang, Z. Zhang, L.H. Kasper, J.E. Lee, C. Wang, P.K. Brindle, Dent SYR, K. Ge, Distinct roles of GCN5/PCAF-mediated H3K9ac and CBP/p300-mediated H3K18/27ac in nuclear receptor transactivation, EMBO J. 30 (2010) 249–262.
[28] Y. Gao, N.V. Gopee, P.C. Howard, L.R. Yu, Proteomic analysis of early response lymph node proteins in mice treated with titanium dioxide nanoparticles, J. Proteom. 74 (2011) 2745–2759.
[29] K.H. Moon, B.L. Hood, B.J. Kim, J.P. Hardwick, T.P. Conrads, T.D. Veenstra, B. J. Song, Inactivation of oxidized and S-nitrosylated mitochondrial proteins in alcoholic fatty liver of rats, Hepatology 44 (2006) 1218–1230.
[30] M.A. Abdelmegeed, S.H. Yoo, L.E. Henderson, F.J. Gonzalez, K.J. Woodcroft, B. J. Song, PPARalpha expression protects male mice from high fat-induced nonalcoholic fatty liver, J. Nutr. 141 (2011) 603–610.
[31] A.W. Tank, H. Weiner, J.A. Thurman, Enzymology and subcellular localization of aldehyde oxidation in rat liver: oxidation of 3,4-dihydroxyphenylacetaldehyde derived from dopamine to 3,4-dihydroxyphenylacetic acid, Biochem. Pharmacol. 30 (1981) 3265–3275.
[32] J.W. Chambers, P.V. LoGrasso, Mitochondrial c-Jun N-terminal kinase (JNK) signaling initiates physiological changes resulting in amplification of reactive oxygen species generation, J. Biol. Chem. 286 (2011) 16052–16062.
[33] D. Sanadi, α-ketoglutarate dehydrogenase from pig heart, Methods Enzymol. 13 (1969) 52–55.
[34] N. Zamzami, G. Kroemer, Methods to measure membrane potential and

permeability transition in mitochondria during apoptosis, Methods Mol. Biol. 282 (2004) 103–116.
[35] P.P. Simeonova, R.M. Gallucci, T. Hulderman, R. Wilson, C. Kommineni, M. Rao, M.I. Luster, The role of tumor necrosis factor-[alpha] in liver toxicity, inflammation, and fibrosis induced by carbon tetrachloride, Toxicol. Appl. Pharmacol. 177 (2001) 112–120.
[36] C. Iida, K. Fujii, T. Kishioka, R. Nagae, Y. Onishi, I. Ichi, S. Kojo, Activation of mitogen activated protein kinase (MAPK) during carbon tetrachloride intoxication in the rat liver, Arch. Toxicol. 81 (2007) 489–493.
[37] M.A. Bae, B.J. Song, Critical role of c-Jun N-terminal protein kinase activation in troglitazone-induced apoptosis of human HepG2 hepatoma cells, Mol. Pharmacol. 63 (2003) 401–408.
[38] C. Latchoumycandane, C.W. Goh, M.M.K. Ong, U.A. Boelsterli, Mitochondrial protection by the JNK inhibitor leflunomide rescues mice from acetaminophen-induced liver injury, Hepatology 45 (2007) 412–421.
[39] N. Hanawa, M. Shinohara, B. Saberi, W.A. Gaarde, D. Han, N. Kaplowitz, Role of JNK translocation to mitochondria leading to inhibition of mitochondria bioenergetics in acetaminophen-induced liver injury, J. Biol. Chem. 283 (2008) 13565–13577.
[40] W.M. Lee, J.R. Senior, Recognizing drug-induced liver injury: current problems, possible solutions, Toxicol. Pathol. 33 (2005) 155–164.
[41] D. Pessayre, B. Fromenty, A. Berson, M.A. Robin, P. Lettéron, R. Moreau, A. Mansouri, Central role of mitochondria in drug-induced liver injury, Drug Metab. Rev. 44 (2012) 34–87.
[42] C.S. Boyer, D.R. Petersen, Hepatic biochemical changes as a result of acute cocaine administration in the mouse, Hepatology 14 (1991) 1209–1216.
[43] J. Henry, K. Jeffreys, S. Dawling, Toxicity and deaths from 3,4-methylenedioxy methamphetamine, Lancet 340 (1992) 384–387.
[44] E.J.M. Pennings, A.P. Leccese, F.A. Wolff, Effects of concurrent use of alcohol and cocaine, Addiction 97 (2002) 773–783.
[45] H. Jaeschke, G.J. Gores, A.I. Cederbaum, J.A. Hinson, D. Pessayre, J.J. Lemasters, Mechanisms of hepatotoxicity, Toxicol. Sci. 65 (2002) 166–176.
[46] C. Ju, Damage-associated molecular patterns: their impact on the liver and beyond during acetaminophen overdose, Hepatology 56 (2012) 1599–1601.
[47] M.A. Abdelmegeed, B.J. Song, Functional roles of protein nitration in acute and chronic liver diseases, Oxid. Med. Cell. Longev. 2014 (2014) 149627.
[48] B.J. Song, M. Akbar, M.A. Abdelmegeed, K. Byun, B. Lee, S.K. Yoon, J. P. Hardwick, Mitochondrial dysfunction and tissue injury by alcohol, high fat, nonalcoholic substances and pathological conditions through post-translational protein modifications, Redox Biol. 3 (2014) 109–123.
[49] J. Bain, H. McLauchlan, M. Elliott, P. Cohen, The specificities of protein kinase inhibitors: an update, Biochem. J. 371 (2003) 199–204.
[50] J. Bain, L. Plater, M. Elliott, N. Shpiro, C.J. Hastie, H. McLauchlan, I. Klevernic, J. S. Arthur, D.R. Alessi, P. Cohen, The selectivity of protein kinase inhibitors: a further update, Biochem. J. 408 (2007) 297–315.
[51] S. Tanemura, T. Yamasaki, T. Katada, H. Nishina, Utility and limitations of SP600125, an inhibitor of stress-responsive c-Jun N-terminal kinase, Curr. Enzym. Inhib. 6 (2010) 26–33.
[52] J. Kim, J. Lee, R. Margolis, R. Fotedar, SP600125 suppresses Cdk1 and induces endoreplication directly from G2 phase, independent of JNK inhibition, Oncogene 29 (2010) 1702–1716.
[53] K.H. Lee, S.E. Kim, Y.S. Lee, SP600125, a selective JNK inhibitor, aggravates hepatic ischemia-reperfusion injury, Exp. Mol. Med. 38 (2006) 408–416.
[54] T.R. Knight, A. Kurtz, M.L. Bajt, J.A. Hinson, H. Jaeschke, Vascular and hepatocellular peroxynitrite formation during acetaminophen toxicity: role of mitochondrial oxidant stress, Toxicol. Sci. 62 (2001) 212–220.
[55] M.A. Abdelmegeed, S. Jang, A. Banerjee, J.P. Hardwick, B.J. Song, Robust protein nitration contributes to acetaminophen-induced mitochondrial dysfunction and acute liver injury, Free Radic. Biol. Med. 60 (2013) 211–222.
[56] S. Kharbanda, S. Saxena, K. Yoshida, P. Pandey, M. Kaneki, Q. Wang, K. Cheng, Y. N. Chen, A. Campbell, T. Sudha, Z.M. Yuan, J. Narula, R. Weichselbaum, C. Nalin, D. Kufe, Translocation of SAPK/JNK to mitochondria and interaction with Bcl-xL in response to DNA damage, J. Biol. Chem. 275 (2000) 322–327.
[57] S. Win, T.A. Than, D. Han, L.M. Petrovic, N. Kaplowitz, c-Jun N-terminal Kinase (JNK)-dependent acute liver injury from acetaminophen or tumor necrosis factor (TNF) requires mitochondrial Sab protein expression in mice, J. Biol. Chem. 286 (2011) 35071–35078.
[58] J. Chambers, L. Cherry, J. Laughlin, M. Figuera-Losada, P.V. Lograsso, Selective inhibition of mitochondrial JNK signaling achieved using peptide mimicry of the Sab kinase interacting motif-1 (KIM1), ACS Chem. Biol. 6 (2011) 808–818.
[59] M.A. Bogoyevitch, B. Kobe, Uses for JNK: the many and varied substrates of the c- Jun *N*-terminal kinases, Microbiol. Mol. Biol. Rev. 70 (2006) 1061–1095.